Coastal Engineering 7 (1983) 41—60
Elsevier Scientific Publishing Company, Amsterdam — Printed in The Netherlands

OPEN-BOUNDARY CONDITIONS FOR OPEN-COAST HURRICANE STORM SURGE

B.A. HARPER and R.J. SOBEY

Hydraulics Laboratory, Public Works Department of New South Wales, Manly Vale, N.S.W. 2093 (Australia)
Department of Civil and Systems Engineering, James Cook University, Townsville Qld. 4811 (Australia)

(Received December 4, 1981; revised and accepted June 11, 1982)

ABSTRACT

Harper, B.A. and Sobey, R.J., 1983. Open-boundary conditions for open-coast hurricane storm surge. Coastal Eng., 7: 41—60.

The specification of realistic open-boundary conditions for the numerical simulation of hurricane (or tropical cyclone) storm surge is considered in the context of the very considerable spatial extent of the meteorological forcing. Existing practice is reviewed and an alternative approach, a Bathystrophic Storm Tide approximation to open-boundary water levels, is presented. Results from a series of numerical experiments demonstrate the advantages of this approach over existing methods.

INTRODUCTION

The meteorological tide forced by a landfalling hurricane (tropical cyclone or typhoon) is reasonably well described by the classical long-wave equations, subject of course to a satisfactory representation of the meteorological forcing. Numerical solutions to these equations, in particular relating to astronomical tide propagation, have been successfully undertaken for several decades now. In many cases also, the extension to storm tides is almost trivial, at least from a numerical viewpoint, although difficulties arise as the spatial extent of the storm tide becomes significant. In the particular case of a hurricane storm tide a conflict of scale develops: at the small end, the storm eye radius together with prominent coastal and bathymetric details must be resolved and, at the large end, the spatial extent of the complete storm. Ideally a computational grid would accommodate both scales of influence — it would be sufficiently large to encompass at all times the spatial extent of a moving tropical cyclone and it would contain sufficient nodal points to adequately represent prominent topographical features and again at all times to describe the steep spatial gradients in the meteorological forcing around the eye wall. Storage

0378-3839/83/0000—0000/$03.00

limitations even on modern time-sharing computer systems largely preclude the adoption of such an extensive computational grid. Indeed this approach would be both inefficient and costly as most interest centres on the smaller scale of motion in the regions of peak, positive and negative, water levels. This paper describes a practical compromise to this conflict of scales in which attention is focussed on the smaller of the two scales and the forcing influence of the tropical cyclone beyond the computational field is included in the open-boundary conditions.

METEOROLOGICAL FORCING AND HYDRODYNAMIC RESPONSE

The tropical cyclone is a large-scale atmospheric disturbance having organised horizontal motion over an area of c. 1500 km in diameter but significant vertical motion only in the lowest few kilometres. The general storm characteristics are well recognised (Fendell, 1974). The tropical cyclone is described as a roughly circular, cyclonic vortex with low-level inflow to, and high-level outflow from, an annular region of intense rainfall, maximum winds and strong updrafts. In the centre is a warm, dry, relatively quiescent core or "eye" which, together with extremely low central pressure (<960 mbar), high central temperature at upper levels (typically 15° C above ambient) and high vortex winds (>40 m/s), distinguishes the mature tropical cyclone from the ordinary tropical depression.

Sea—air interaction is described in terms of the near-surface wind and pressure fields. Typical radial profiles through a storm are shown in Fig. 1. The M.S.L. atmospheric pressure exhibits almost an axisymmetric vee structure, dropping rapidly towards the centre through the eye wall to the storm central pressure p_o, which itself is often adopted as a single measure of storm intensity. Beyond the eye wall the profile approaches moderately rapidly to ambient pressure levels. The spatial distribution of the sustained azimuthal

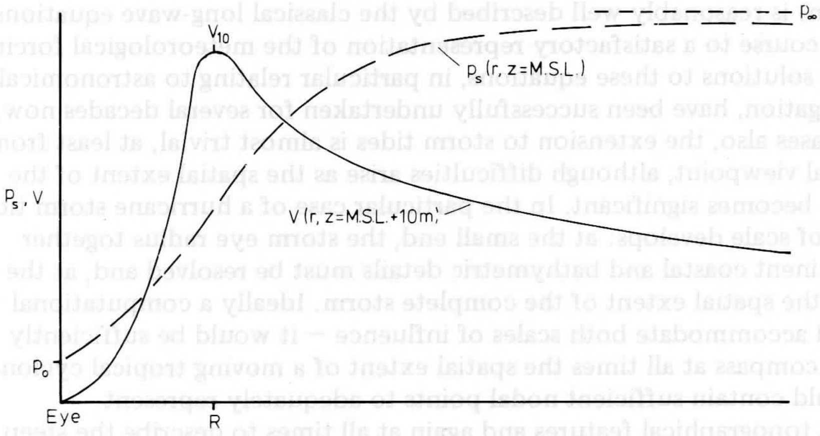

Fig. 1. Typical wind velocity and atmospheric pressure profiles within a tropical cyclone.

(or tangential) wind speed at height 10 m has a significant asymmetry stemming largely from the storm forward motion but the dominant features remain as indicated in Fig. 1. From the quiescent zone at the storm centre the wind speed increases rapidly towards a maximum around the eye wall and then decays away towards the storm periphery at a mild rate. As a result, there remains substantial wind forcing at distances from the storm centre measured in the low hundreds of kilometers. The atmospheric boundary layer of course results in a wind-induced shear stress τ_s on the water surface, which appears directly in the long-wave equations together with the M.S.L. atmospheric pressure p_s. The distance from the eye to the position of maximum wind velocity is termed the radius to maximum winds R, a parameter that is adopted almost exclusively as a measure of the spatial scale of the storm. R is typically in the range 20 to 40 km.

In deep water away from coastal effects the total storm tide is predominantly a response to pressure forcing. The M.S.L. atmospheric pressure structure of the storm induces a superelevated mound of water, the so-called inverse barometer effect, that broadly mirror images the pressure profile for a stationary storm. An hydrostatic approximation to the local magnitude of the pressure surge is:

$$\Delta B = \frac{p_\infty - p_s}{\rho_w \, g} \tag{1}$$

where p_s is the local M.S.L. atmospheric pressure, p_∞ is the ambient pressure at the extremities of the storm and ρ_w is the mass density of sea water; ΔB amounts to approximately a 1 cm rise per 1 mbar pressure drop and is independent of the water depth. As the storm moves, dynamic effects become more important, particularly over the continental shelf.

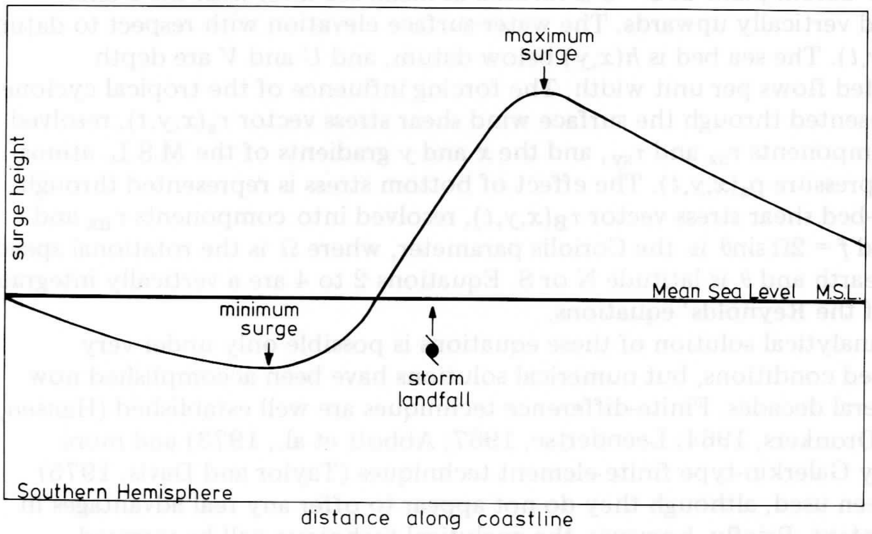

Fig. 2. Typical coastal surge profile.

For a landfalling tropical cyclone the near-circular surface wind field (clockwise in the Southern Hemisphere) is responsible for the greater part of the surge at the coast where levels reach their peak. Large-scale water circulations are established over the continental shelf as the cyclone approaches land, resulting in the characteristic coastal storm surge profile shown in Fig. 2 for a Southern Hemisphere location. With the observer facing seawards, predominantly onshore winds to the right of the storm path force water towards the coast (setup), while offshore winds to the left force water away from the shore causing a decrease in sea level (setdown or drawdown). Storm characteristics, major topographical features and even the simultaneous astronomical tide can all substantially influence surge behaviour, but the general trend indicated by Fig. 2 for coastal water levels persists.

PROPAGATION OF A DISTURBANCE

The classical long-wave equations (Welander, 1964) describing the conservation of mass and momentum in two spatial directions x and y are:

$$\frac{\partial \eta}{\partial t} + \frac{\partial U}{\partial x} + \frac{\partial V}{\partial y} = 0 \qquad (2)$$

$$\frac{\partial U}{\partial t} + \frac{\partial}{\partial x}\frac{(U^2)}{h+\eta} + \frac{\partial}{\partial y}\frac{(UV)}{h+\eta} - fV = -g(h+\eta)\frac{\partial \eta}{\partial x} - \frac{(h+\eta)}{\rho_w}\frac{\partial p_s}{\partial x} + \frac{1}{\rho_w}(\tau_{sx} - \tau_{Bx}) \qquad (3)$$

$$\frac{\partial V}{\partial t} + \frac{\partial}{\partial x}\frac{(UV)}{h+\eta} + \frac{\partial}{\partial y}\frac{(V^2)}{h+\eta} + fU = -g(h+\eta)\frac{\partial \eta}{\partial y} - \frac{(h+\eta)}{\rho_w}\frac{\partial p_s}{\partial y} + \frac{1}{\rho_w}(\tau_{sy} - \tau_{By}) \qquad (4)$$

The x-y datum plane at $z = 0$ is located at mean sea level with the z axis directed vertically upwards. The water-surface elevation with respect to datum is $\eta(x,y,t)$. The sea bed is $h(x,y)$ below datum, and U and V are depth integrated flows per unit width. The forcing influence of the tropical cyclone is represented through the surface wind shear stress vector $\tau_s(x,y,t)$, resolved into components τ_{sx} and τ_{sy}, and the x and y gradients of the M.S.L. atmospheric pressure $p_s(x,y,t)$. The effect of bottom stress is represented through the sea-bed shear stress vector $\tau_B(x,y,t)$, resolved into components τ_{Bx} and τ_{By}, and $f = 2\Omega \sin\theta$ is the Coriolis parameter, where Ω is the rotational speed of the earth and θ is latitude N or S. Equations 2 to 4 are a vertically integrated form of the Reynolds' equations.

An analytical solution of these equations is possible only under very restricted conditions, but numerical solutions have been accomplished now for several decades. Finite-difference techniques are well established (Hansen, 1956; Dronkers, 1964; Leendertse, 1967; Abbott et al., 1973) and more recently Galerkin-type finite-element techniques (Taylor and Davis, 1975) have been used, although they do not appear to offer any real advantages in this context. Briefly, however, the analytical technique will be pursued.

Equations 2 to 4 are reduced to their primitive form by neglecting convective and Coriolis accelerations and bed resistance, by generalising the meteorological forcing and by assuming constant water depth and small-amplitude waves. The equations may then be recast as the non-homogeneous wave equation in two space dimensions:

$$\frac{\partial^2 \eta}{\partial t^2} = C^2 \left(\frac{\partial^2 \eta}{\partial x^2} + \frac{\partial^2 \eta}{\partial y^2} \right) + Q \tag{5}$$

where $C = \sqrt{gh}$ is the wave celerity and $Q(x,y,t)$ is the generalised representation of the meteorological forcing. Physically, eq. 5 describes the radial propagation in space at speed C of any disturbance, either existing at zero time or subsequently introduced by the continuation of the meteorological forcing Q after time zero. Such disturbances, although modified and perhaps attenuated by effects that have been omitted from eq. 5, clearly persist in time and propagate to infinity. For a typical continental shelf depth of 50 m the propagation speed would be 22 m/s, a not inconsiderable speed which illustrates the complex and rapid large-scale interactions that characterise a hurricane storm tide. It follows in general that the solution domain must extend to infinity in space, at least from a theoretical viewpoint. However any numerical solution technique, be it numerical integration of eq. 5 or more appropriately a finite-difference or finite-element solution of the long-wave equations, requires a finite-solution domain. At the limits of this domain, boundary conditions must be specified to represent the influence of all disturbances propagating into the domain from outside. In its mathematical sense, of course, the truncated solution domain must be simply connected.

The resulting boundary conditions are of two types, respectively closed- and open-boundary conditions. Solid land is a closed boundary; no disturbance can propagate through such a boundary and this is transmitted to the solution domain by specifying zero normal flow at such positions. In most long-wave situations, including hurricane storm surges, the finite-solution domain is completed by a length of open boundary through which water may flow and waves or disturbances may propagate. The numerical solution requires that open-boundary conditions be specified along such boundaries. This is by no means a trivial problem.

EXISTING PRACTICE

Astronomical tide propagation has received considerable attention and it is useful to briefly consider this related problem. A typical problem involves the tidal flow in a bay or wide estuary. A length of open boundary is defined across the bay or estuary mouth along which the ocean tide is specified at all times. If the Q in eq. 5 is now taken to represent gravitational forcing (a body force) rather than meteorological forcing (a surface force), then the practice outlined above is equivalent to assuming that gravitational forcing (i.e. Q) is zero within the solution field and that the entire influence of gravitational forcing outside the computational field is included in the open boundary conditions, at least as far as the solution field is concerned. The apparent success of numerical hydrodynamic models of astronomical tide propagation indicates that this approach is quite reasonable in its context, at least where the spatial extent of the solution field is not too extensive.

It is clear that such a convenient situation does not exist for meteorological tides, in particular hurricane storm surge. Forcing in the general vicinity of the storm eye is the dominant influence and must be included. Forcing outside a typical solution field has a secondary role but is physically significant; it must be included in the open-boundary conditions. Here again the situation is more complicated than for astronomical tides. The latter are periodic and the water-level history at any site is readily predicted for any past or future time from an harmonic analysis of limited field observations at the particular site. Storm tides, however, are transient waves and the water level history at any site cannot be separately predicted as a time series.

Published details on existing practice for meteorological tides are not numerous. There is some information on storm tides in enclosed or semi-enclosed water bodies (Tokyo Bay, Galveston Bay, Lake Michigan, Manila Bay) where internal forcing is assumed dominant and open-boundary conditions are not a significant problem. The true open-coast situation is where the problems arise and where open-boundary conditions can have an identifiable impact on the computed solution. In plan and schematic forms the situation is illustrated in Fig. 3 and 4 for a Southern Hemisphere, east coast site with a tropical cyclone travelling westwards across the continental shelf. For computational efficiency the solution field is normally rectangular, fixed in space and aligned longitudinally (y direction) along the general run of the coastline. The upper (BC), lower (AD) and right-hand (CD) sides of the rectangle are the open boundaries along which suitable boundary conditions must be specified. In terms of this computational field a "landfalling" tropical cyclone is a storm whose track enters the field across the right-hand open boundary and leaves across the left-hand closed boundary. The right-hand boundary is typically located in very deep water beyond the edges of the continental shelf, as indicated in Fig. 4. For the upper and lower boundaries, water depths decrease rapidly from the edge of the continental shelf to the shoreline.

A series of pioneering papers by Jelesnianski (1965, 1972, 1974) has considered the open-coast hurricane storm surge problem in reasonable detail, identifying the dominant physical processes involved in the generation and propagation of the surge wave. Numerical hydrodynamic modelling was adopted as the basic approach but the overall objectives were limited to the provision of reasonably reliable surge forecasts at a nominated open coast site. The model basin dimensions are standardised at 600 statute miles alongshore (y direction) by 72 statute miles offshore (x direction), the latter distance being typical of continental shelf widths for the Atlantic and Gulf of Mexico

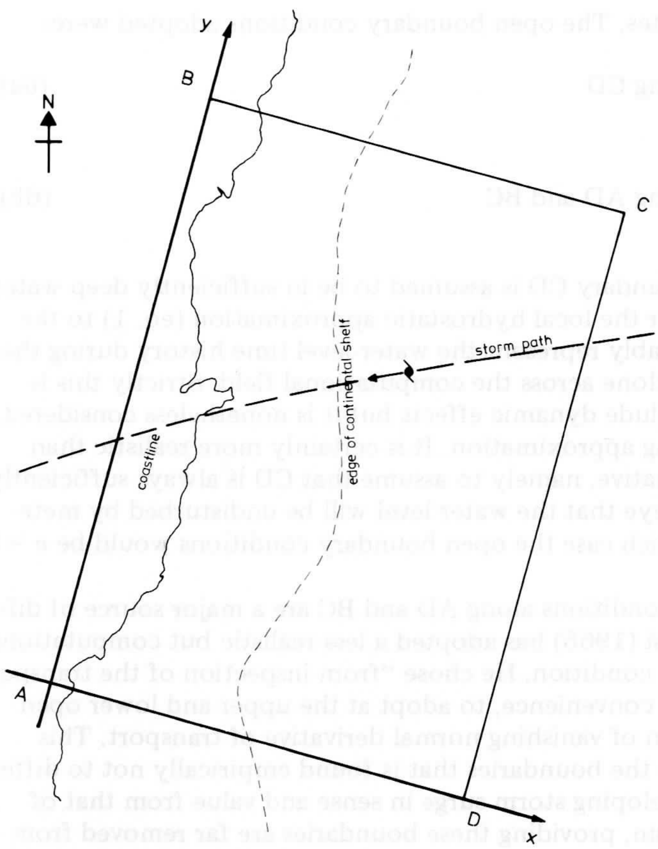

Fig. 3. Open coast situation.

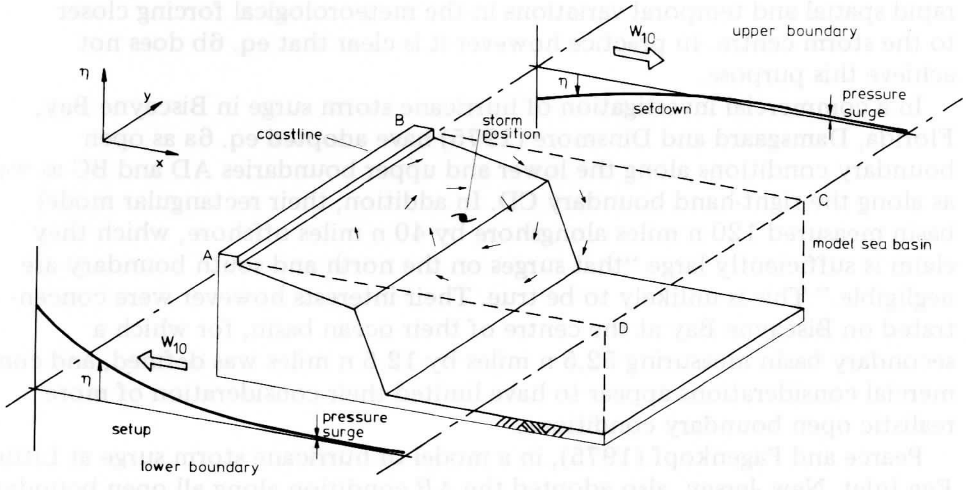

Fig. 4. Concept of Bathystrophic Storm Tide open-boundary condition.

coasts of the United States. The open boundary conditions adopted were:

$$\eta = \Delta B \qquad \text{along CD} \qquad (6a)$$

and

$$\frac{\partial V}{\partial y} = 0 \qquad \text{along AD and BC} \qquad (6b)$$

The right-hand open boundary CD is assumed to be in sufficiently deep water throughout its length for the local hydrostatic approximation (eq. 1) to the pressure surge to reasonably represent the water-level time history during the passage of a tropical cyclone across the computational field. Strictly this is not true as it fails to include dynamic effects but it is nonetheless considered a satisfactory engineering approximation. It is certainly more realistic than the only apparent alternative, namely to assume that CD is always sufficiently distant from the storm eye that the water level will be undisturbed by meteorological effects, in which case the open boundary conditions would be $\eta = 0$ (Heaps, 1969).

The open-boundary conditions along AD and BC are a major source of difficulty. Here Jelesnianksi (1965) has adopted a less realistic but computationally convenient boundary condition. He chose "from inspection of the transport field, and as a matter of convenience, to adopt at the upper and lower open boundaries the condition of vanishing normal derivative of transport. This permits transport across the boundaries that is found empirically not to differ radically during the developing storm surge in sense and value from that of a much larger closed basin, providing these boundaries are far removed from the storm centre." In spirit this boundary condition attempts to represent a distant asymptotic state where the flow pattern is uninfluenced by the rapid spatial and temporal variations in the meteorological forcing closer to the storm centre. In practice however it is clear that eq. 6b does not achieve this purpose.

In a commercial investigation of hurricane storm surge in Biscayne Bay, Florida, Damsgaard and Dinsmore (1975) have adopted eq. 6a as open boundary conditions along the lower and upper boundaries AD and BC as well as along the right-hand boundary CD. In addition, their rectangular model basin measured 120 n miles alongshore by 40 n miles offshore, which they claim is sufficiently large "that surges on the north and south boundary are negligible." This is unlikely to be true. Their interests however were concentrated on Biscayne Bay at the centre of their ocean basin, for which a secondary basin measuring 52.5 n miles by 12.5 n miles was defined, and commercial considerations appear to have limited their consideration of more realistic open boundary conditions.

Pearce and Pagenkopf (1975), in a model of hurricane storm surge at Little Egg Inlet, New Jersey, also adopted the ΔB condition along all open boundaries with an additional constraint that there is no flow along the upper and lower boundaries. Specifically their open-boundary conditions were

$$\eta = \Delta B \qquad \text{along CD} \tag{7a}$$

and

$$\eta = \Delta B, \quad U = 0 \qquad \text{along AD and BC} \tag{7b}$$

They recognised that the "proximity of the lateral boundaries to the zone of high wind stress may significantly effect the calculated surge heights and corresponding current velocities." They conducted sensitivity studies to determine an optimum lateral grid size (i.e. the distance CD) for a specific storm, based on the peak surge height at one point, Little Egg Inlet, only. Their final rectangular model basin measured 260 n miles alongshore and 118 n miles offshore, having only a 1% influence on the peak surge at Little Egg Inlet for a specific storm. The rationale for the $U = 0$ constraint on the upper and lower boundaries is not discussed but in spirit at least it is related to the distant asymptotic state sought also by Jelesnianski.

AN ALTERNATIVE PROPOSAL

The major difficulty from a physical and mathematical viewpoint is the open boundary conditions along the upper and lower boundaries AD and BC. Although these boundaries are some distance from the storm track there remains substantial wind forcing, as previously indicated; the result is illustrated on Fig. 2 and in more detail on Fig. 4. Along the lower boundary AD the wind is predominantly onshore. There is a superelevation in deep water at D that is almost entirely pressure surge ΔB. The onshore winds active on the shallower waters of the continental shelf force a setup of water against the coast, substantially increasing the superelevation above normal water level in the manner indicated in Fig. 4. Along the upper boundary BC the situation is almost reversed. The superelevation in deep water at C corresponding to the pressure surge ΔB remains but the predominantly offshore winds along BC force a setdown of water levels at the coast below normal water level, again in the manner illustrated in Fig. 4. It is these contrasting conditions along the upper and lower boundaries that must be transmitted to a numerical model. Failure to do so certainly limits the usefulness of any computed solution in the vicinity of the open boundaries and potentially also throughout the solution field.

In a recent numerical hydrodynamic model study of tropical cyclone storm surge, the present writers (Harper et al., 1977; Sobey et al., 1977, 1982) have adopted an alternative boundary condition that attempts to represent just these conditions, potentially enhancing the predictive capabilities of the entire solution field. It may be termed the Bathystrophic Storm Tide or B.S.T. approximation. The open-boundary water levels are set equal to the local bathystrophic storm tide, the quasi-steady profile along the open boundary computed on the assumption that the lowest-order momentum balance at the boundary is in fact directed along the boundary. It is further assumed that the spatial distribution of the atmospheric pressure gradient and wind shear stress along the open boundary is held constant at values appropriate for the new time. The inertial terms are ignored in the lowest order balance, which is equivalent to assuming that the steady state is achieved over a single time step, an assumption that is open to some question. The time scale to achieve a quasi-steady state in response to a sustained change in the forcing is the frictional decay time $8h^2/\lambda|U|$, where λ is the Darcy-Weisbach friction factor. This frictional decay time is typically six hours for the continental shelf, but much smaller in shallower water where the open-boundary conditions are more critical. The common adoption of $\eta = \Delta B$ as a deep-water open-boundary condition involves a similar but even more questionable assumption as the frictional decay time is very long in deep water.

Coriolis accelerations have also been omitted from the lowest-order momentum balance and some appreciation of this assumption is possible from a comparison of the time scales of the contributing processes. The time scale of the forced long wave response is R/V_{FM}, where V_{FM} is the forward speed of the eye, and is typically two hours. The inertial time scale, the time scale for Coriolis accelerations to influence the forced response, is $2\pi/f$, which is typically thirty-six hours at hurricane latitudes. The bathystrophic storm tide terminology introduced above normally refers to a one-dimensional approach where Coriolis terms are included. Coriolis accelerations can be retained without difficulty (and have been in exploratory computations) but it is quite clear from the response times that they have little influence on hurricane storm surge on the continental shelf. The B.S.T. terminology has nonetheless been retained, despite the omission of the Coriolis accelerations, as there is little essential difference in the present context and as it is commonly identified as a one-dimensional approach.

Under such assumptions the steady-state profile is described by a reduced form of eq. 3:

$$0 = -g(h+\eta)\frac{\partial \eta}{\partial x} - \frac{(h+\eta)}{\rho_w}\frac{\partial p_s}{\partial x} + \frac{\tau_{sx}}{\rho_w} \tag{8}$$

The partial derivatives may now be written as ordinary derivatives and the equation rephrased as the first-order ordinary differential equation:

$$\frac{d\eta}{dx} = -\frac{1}{\rho_w g}\frac{dp_s}{dx} + \frac{\tau_{sx}}{\rho_w g(h+\eta)} \tag{9}$$

The pressure gradient and wind shear stress on the right-hand side are determined by the wind and pressure structure of the moving hurricane, the depth h by the offshore bathymetry. All three of these quantities vary with position and the right-hand side of eq. 9 is completely defined for all x along the open boundary. Numerical integration of this equation at each time step from deep water to the coast yields the local Bathystrophic Storm Tide, which is proposed as a suitable dynamic open-boundary condition along the upper and lower boundaries. Initial conditions in deep water at C or D are $\eta = \Delta B$ and the numerical integration can be performed efficiently by the Runge-Kutta method or some similar algorithm. This boundary condition readily reproduces wind setup and setdown in the manner indicated in Fig. 4 and has been extensively utilised by the present writers in a series of tropical cyclone storm surge simulations at twelve separate sites along Australia's northeastern and northwestern coastline (Harper et al., 1977). Equation 6a was adopted in these simulations to represent the open boundary conditions along the deep water open boundary CD.

It is clear from eq. 5 that the B.S.T. condition (eq. 9), along with the hydrostatic pressure surge condition (eq. 6a) and the asymptotic flow condition (eq. 6b), all fail to completely describe the respective open boundary conditions. The B.S.T. condition however is proposed as a satisfactory engineering approximation to real water-level conditions along the upper and lower open boundaries.

EVALUATION OF ALTERNATIVE PROPOSALS

A definitive choice among the alternative open boundary proposals is not possible at present. No appropriate analytical solution is available against which numerical solutions within a truncated solution domain may be evaluated. Field data that are available amount to little more than a handful of water-level time histories recorded by permanently installed tide gauges, grossly insufficient for even a satisfactory model calibration. A careful evaluation of numerical simulations under comparable conditions remains the only avenue for guidance in the choice of the most appropriate proposal. Figure 5 summarises the open-boundary alternatives which were considered. In addition, the M.S.L. condition ($\eta = 0$) along all open boundaries has been included for comparison. The outer open boundary CD is not presented here because the various open boundary conditions differ only slightly in this regard, and have little or no influence on coastal water levels.

For comparative purposes an idealised test basin broadly representative of conditions along northeastern Australia's continental shelf has been adopted. The basin is a coastal area with a straight coastline running north to south and positioned at an east coast site at 19° S latitude. The area covered extends a distance of 195 n miles (361 km) along the coast and a distance of 145 n miles (269 km) seaward into the Coral Sea. The basin bathymetry varies only in the offshore direction, the cross-section being illustrated in Fig. 4. The sea-bed profile has a constant slope of 0.0008 from a depth of 4 m below M.S.L. at the coast to a distance of 120 km offshore, at which point the water depth is 100 m below M.S.L.. To represent

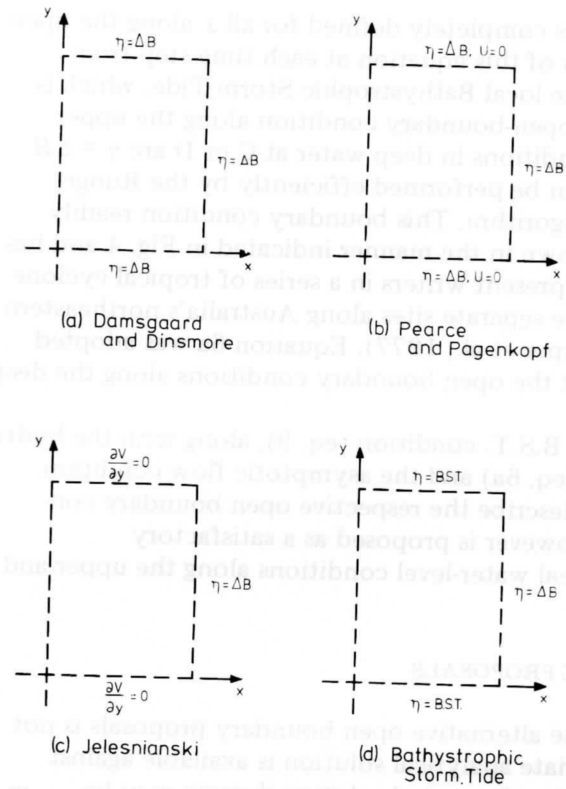

Fig. 5. Open-boundary alternatives.

the sudden drop from the edge of the continental shelf to the depths of the Coral Sea, the bed slope dips at a steep 0.02 for the next 20 km, with depths beyond 140 km considered constant at 500 m below M.S.L.. Actual Coral Sea depths are much deeper (of order 2000 m) but this has little influence on surge wave development.

Tropical cyclone storm surge generation and propagation within this truncated solution domain is described by the long-wave equations 2 to 4. The numerical hydrodynamic model SURGE based on these equations and developed by the present writers is described in detail elsewhere (Sobey et al., 1977, 1982). It is based on an explicit finite difference scheme similar to that adopted by Reid and Bodine (1968). The wind and pressure structure of the moving tropical cyclone is based essentially on the recommendations of Graham and Nunn (1959) and the wind stress relationships follow the recommendations of Wu (1969). This model has been adopted for the purposes of numerical experiment within the idealised test basin, the solution domain being covered by a 30 by 40 square matrix of grid points with a 5-n mile (9.3 km) grid spacing.

A standard storm based on the characteristics of tropical cyclone "Althea" has been adopted. "Althea", which crossed the Queensland coast near Townsville in December 1971, is one of the best documented storms in Australia. Its major characteristics, in terms of the parameters discussed earlier, are listed in Table I.

TABLE I

Characteristics of the standard storm

Central presure	p_o	950 mbar
Ambient pressure	p_∞	1013 mbar
Max. sustained wind	V_{10}	45 m/s
Radius to max. wind	R	35 km
Forward speed of eye	V_{FM}	20 km/hr

For each of the following open boundary experiments, the storm is initially situated at the centre of the test basin in the deep water area with a quiescent flow field and all water levels set to M.S.L. Over a period of 4 hours the storm is held stationary and its intensity (i.e. wind speed and pressure deficit) is gradually increased from zero to the full values following a sine curve with period 8 hours from a trough to the following crest. This procedure effectively eliminates, for this basin, the transient-free waves which result from a sudden application of the forcing. After the storm reaches full intensity, it is moved perpendicularly to and towards the coastline at the constant speed V_{FM}. Landfall is made 7 hours later and simulation continues for a further 3 hours after landfall as the storm moves inland.

Output from SURGE is presented as water level profiles along the coastline AB and along the upper BC and lower AD open boundaries at the simulation times −6, −3, −1, 0, +1 and +3 hours with respect to the time of storm landfall. In addition, water level time histories are presented at coastal locations named MIN, EYE and MAX, being respectively close to the point of maximum drawdown, beneath the path of the storm eye and in the vicinity of the maximum surge level as shown in Fig. 9. Together these locations represent the major features of storm surge response at the coastline. Finally, some comparisons are made on the basis of water-level contour patterns throughout the solution field.

DISCUSSION OF RESULTS

Not unexpectedly perhaps, little difference was found between the results obtained from the Damsgaard and Dinsmore (eq. 6a) and the Pearce and Pagenkopf (eq. 7) boundary conditions. The $U = 0$ condition imposed by Pearce and Pagenkopf leads to slightly lower water levels at the coast immediately adjacent to the open boundaries, but otherwise these results are almost identical. As a consequence, the Damsgaard and Dinsmore condition has been excluded from the comparisons presented below.

The coastal water-level comparisons are presented in Fig. 6. There is general agreement regarding the broad characteristics of the coastal profiles but there are some important differences in detail that are not restricted to the immediate vicinity of the boundaries but extend throughout the solution field. The locations of peak setup and setdown do not seem to be affected by the boundary conditions but actual water levels vary over a range of about 0.5 m.

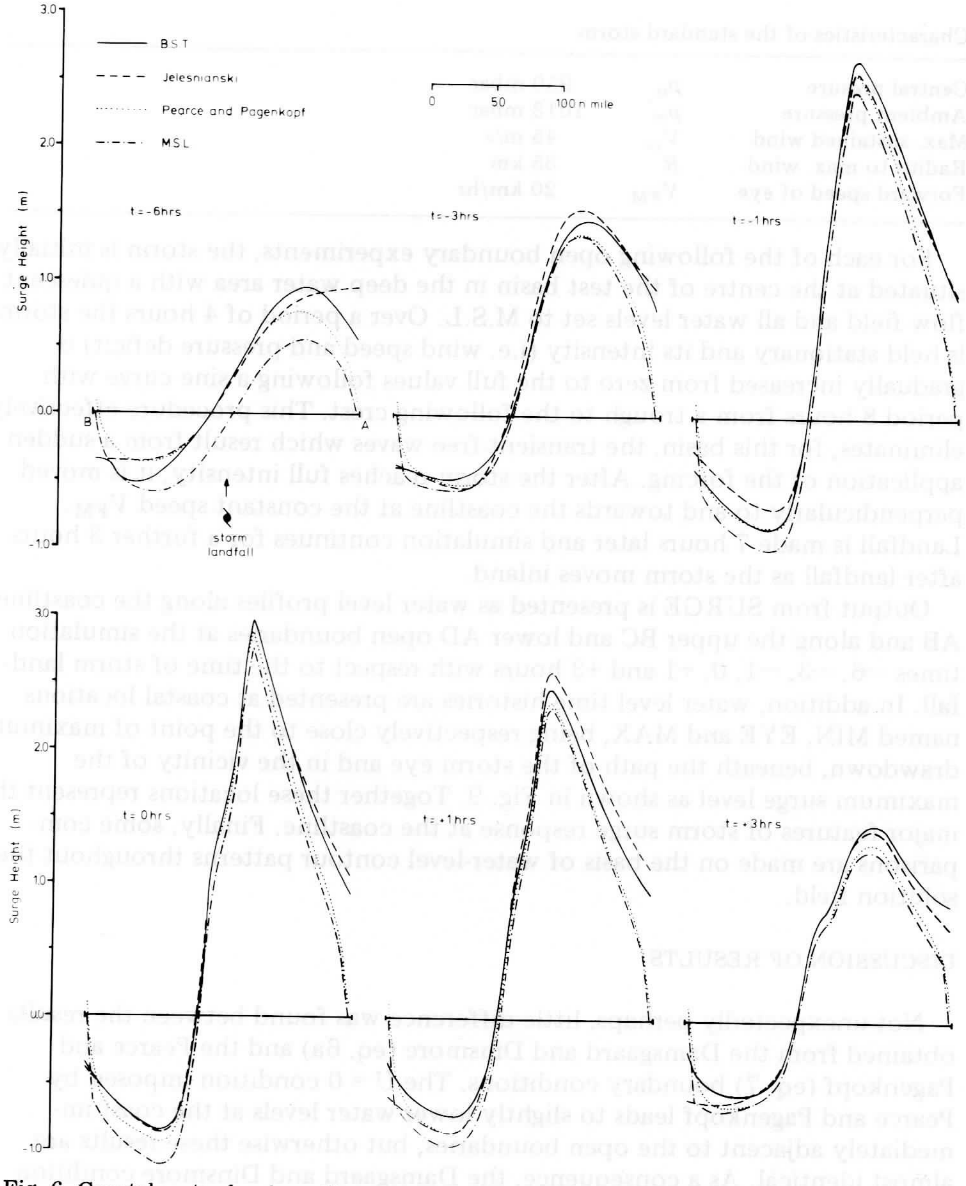

Fig. 6. Coastal water-level profiles.

The differences tend to become smaller as the intensity of the forcing increases but the influence of the boundary conditions is quite clear at all times. The M.S.L. condition forces consistently lower water levels throughout, with both a larger setdown and a smaller setup. The Pearce and Pagekopf/Damsgaard and Dinsmore boundary conditions displace the M.S.L. coastal profiles upwards as expected, more water having been forced into the solution field, but the change varies with time and position. Coastal water levels differ by about 0.25 m at −6 hrs. This difference persists around the maximum setdown position but decreases around the peak setup position during storm passage.

The response to the B.S.T. boundary conditions conformed with expectations. The increased setup at the lower open boundary further increased the water levels around the peak setup position, the difference from the M.S.L. results being about 0.4 m at −6 hrs, reducing to about 0.25 m during storm passage across the shelf. This pattern is initially reversed around the maximum setdown position, which is closer to the upper open boundary where offshore winds force a setdown on top of the barometric setup. At −6 hrs the B.S.T. result is closer to the M.S.L. result than to the Pearce and Pagenkopf result but the setdown decreases as the storm crosses the shelf. By the time of storm landfall, the lower boundary setup has become the dominant influence and the predicted drawdown is smaller by about 0.2 m for the duration of the run. Figure 6 gives an excellent overall impression of the impact of the B.S.T. boundary conditions, which is to increase the peak surge level and to decrease the setdown levels just before and after storm landfall. From a physical viewpoint there is little doubt that these trends are realistic. The relative magnitude of the change from the M.S.L. result is quite instructive. The lower boundary setup reaches about 1.0 m but the peak surge is only increased by about 0.25 m, which tends to generate confidence in the capacity of the B.S.T. boundary conditions to represent meteorological forcing beyond the open boundaries.

The surprise results on Fig. 6 are those derived from the Jelesnianski boundary conditions. The coastal profile response is reasonably close to the B.S.T. results, with setup at the lower boundary and setdown at the upper boundary. There are significant differences however at the beginning and end of the run that do not seem to be consistent with physical expectations.

This point is much clearer in Fig. 7 which shows water level profiles along the upper and lower boundaries during storm passage for the B.S.T. and Jelesnianski boundary conditions. Both boundary conditions produce setdown at the upper boundary and setup at the lower boundary but the differences during the early and later stages of simulation are quite significant. The B.S.T. condition shows lower boundary setup building during storm approach to a peak of about 1.0 m at about −1 hrs, where it is held by inertial forces for several hours. The Jelesnianski boundary conditions force a coastal setup of order 1.0 m at −6 hrs, which is maintained until about two hours after landfall when it begins to fall rapidly. Upper-boundary setdown levels forced by the B.S.T. condition remain approximately constant at about 0.4 m

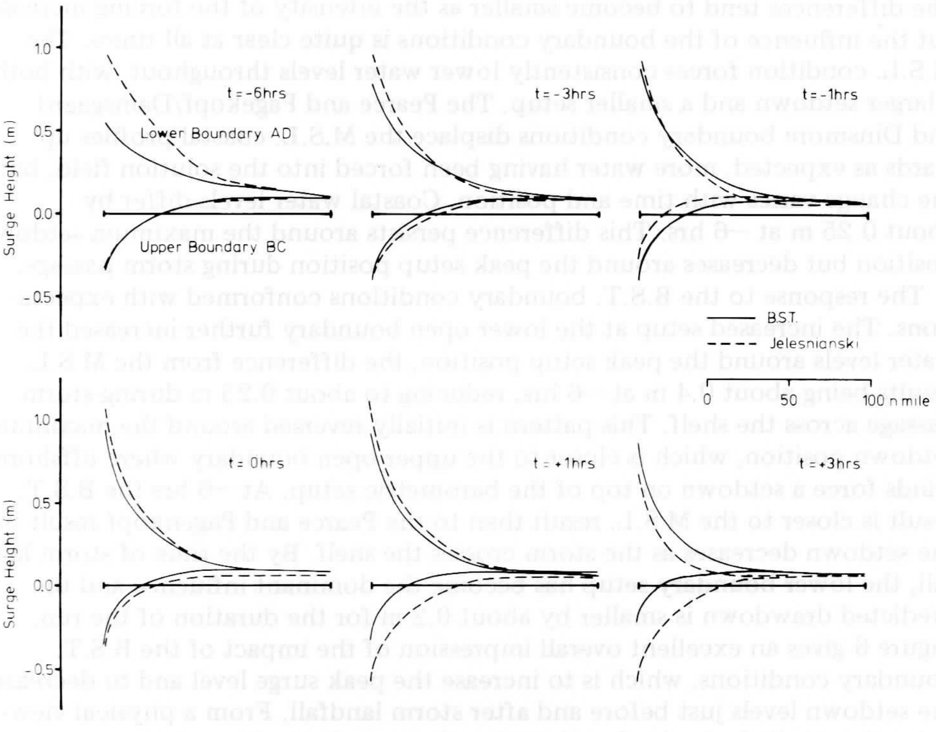

Fig. 7. Water-level profiles along the upper and lower open boundaries.

until storm landfall, after which there is a gradual decay. The Jelesnianski results are initially similar but decrease before storm landfall to about 0.25 m, recover to about 0.4 m at landfall and increase to about 0.6 m for several hours after landfall. It is difficult to rationalise the differences, especially at the beginning and end of the simulation runs. The B.S.T. boundary conditions respond as expected, with coastal water levels building with the storm forcing. The shape of the Jelesnianski boundary profiles certainly conform with physical expectations but the time history of the magnitudes seem to bear little relationship to the forcing at the beginning and end of the simulation.

The water level time histories at the coastal locations MIN, EYE and MAX shown in Fig. 8 are generally consistent in magnitude with the Fig. 6 results. Two waves are apparent, both moving northwards along the continental shelf. The lower amplitude initial wave appears to be a free mode, probably a shelf wave forced by the storm initialisation, and is of little importance in the present context. The larger amplitude wave is the forced surge wave. The trends are generally quite similar but the influence of the boundary conditions is still apparent. As observed in Fig. 6, the M.S.L. and Pearce and Pagenkopf boundary conditions yield lower peak surge levels but their peaks are approximately in phase with the B.S.T. result. The Jelesnianski result, however, shows a phase lag of about 15 mins at MIN and MAX but not at EYE. Once again it

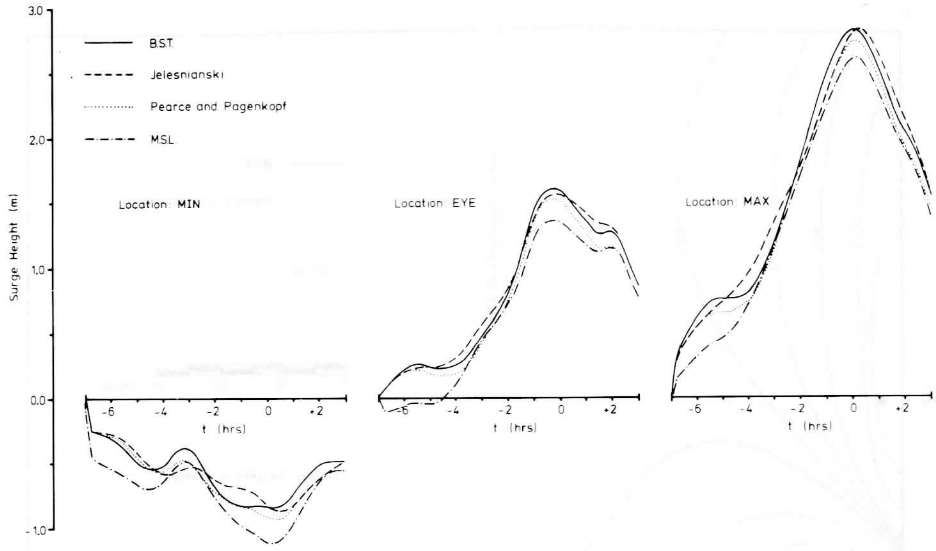

Fig. 8. Water-level histories at the coastline.

is the B.S.T. result that most closely conforms to physical expectations throughout.

Figure 9 is included to contrast the different open-boundary conditions. It compares the water-level contour patterns produced by the B.S.T. and Pearce and Pagenkopf conditions over the entire solution field at the time of storm landfall. The dominant features are the extensive area of water level setup south of the storm path and the less extensive area of setdown to the north. Most of the setup/setdown is contained within the continental shelf. The influence of the B.S.T. open-boundary condition is seen here to advantage, the water-level contours continuing on to intersect the open boundaries. The Pearce and Pagenkopf condition constrains the contours to the coastline at the upper and lower boundaries, forcing higher water-level gradients and hence velocities in these regions.

CONCLUSIONS

Some compromise is unavoidable in modelling open coast storm surge to a scale of the order of the radius of maximum winds and simultaneously including the area of significant surge generation. As the solution domain must be truncated, it is important that the meteorological forcing outside the domain be represented in the open-boundary conditions.

Of the five alternative proposals considered, the M.S.L. condition offers no advantages, is nonconservative in effect and is not recommended. The next most effective proposals are those of Pearce and Pagenkopf and Damsgaard and Dinsmore, where the local hydrostatic approximation to the pressure surge is

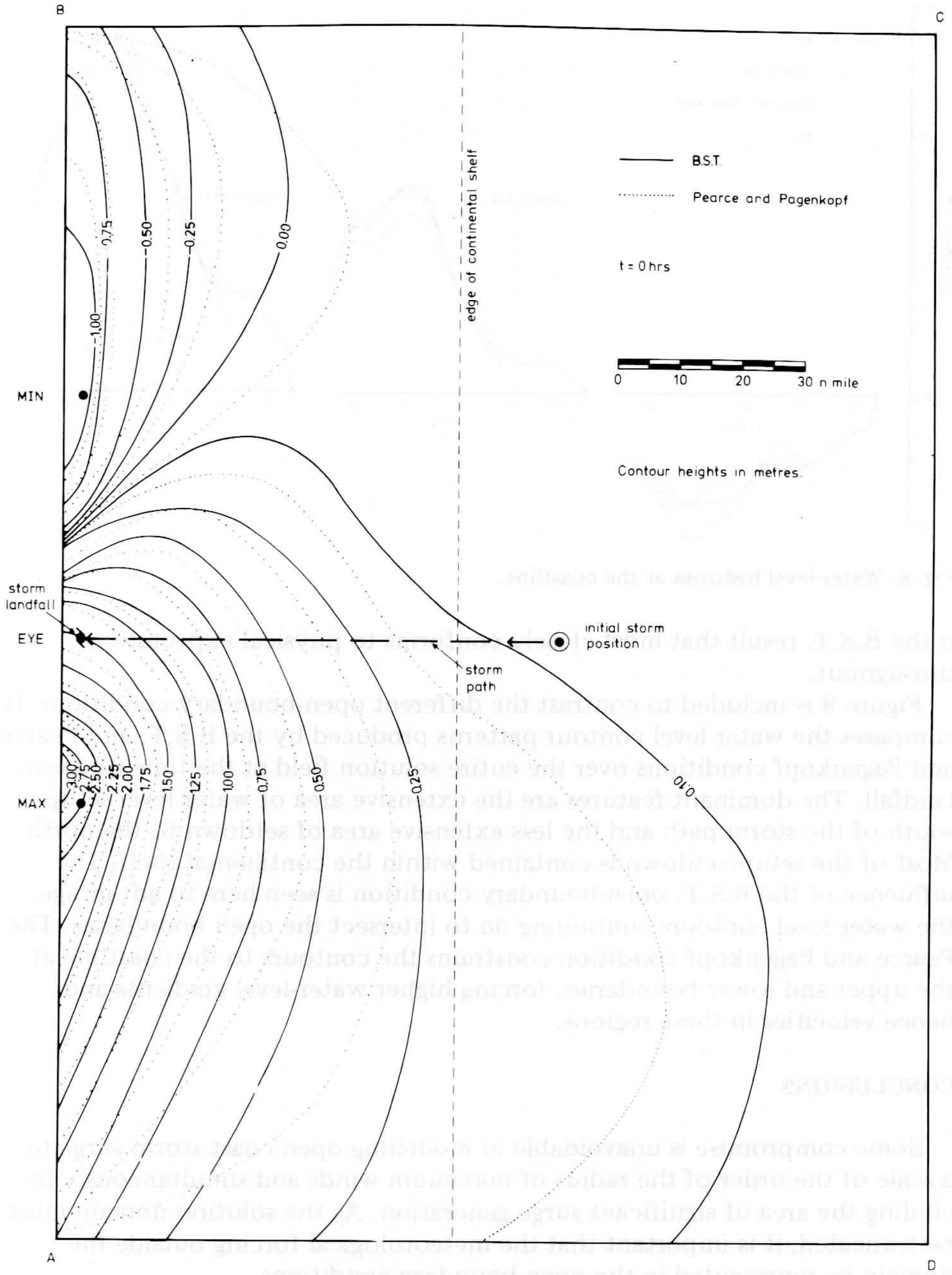

Fig. 9. Water-level contour patterns.

used as the open-boundary condition. These methods do not give realistic water levels in close proximity to the open boundaries and the effective yield of the solution field is reduced. The Jelesnianski asymptotic flow condition yields open boundary profiles that follow the correct trends but the levels appear unrelated to the storm forcing at the beginning and end of simulation. A B.S.T. condition is proposed as a suitable open boundary condition. This boundary condition is closely related to the hydrodynamics, responds realistically to storm forcing and also gives realistic water-level contour and flow patterns close to the open boundaries.

Finally, the actual peak surge is relatively insensitive to the open-boundary conditions, with the exception of the M.S.L. condition. The differences would become much more significant however for a smaller solution field.

REFERENCES

Abbott, M.B., Damsgaard, A. and Rodenhuis, G.S., 1973. System 21, 'Jupiter' (A design system for two-dimensional nearly-horizontal flows). J. Hydraulic Res., 11: 1—28.

Damsgaard, A. and Dinsmore, A.F., 1975. Numerical simulation of storm surges in bays. Proc. Symposium on Modeling Techniques, ASCE, San Francisco, pp. 1535—1551.

Dronkers, J.J., 1964. Tidal Computations in Rivers and Coastal Waters. North Holland, Amsterdam.

Fendell, F.E., 1974. Tropical cyclones. Adv. Geophys., 17: 1—100.

Garabedian, P.R., 1964. Partial Differential Equations. John Wiley and Sons, New York, N.Y., 672 pp.

Graham, H.E. and Nunn, D.E., 1959. Meteorological considerations pertinent to standard project hurricane, Atlantic and Gulf Coasts of the United States. U.S. Weather Bureau, National Hurricane Research Project, Report No. 33.

Hansen, W., 1956. Theorie zur Errechnung des Wasserstandes und der Stromungen in Randmeeren nebst Anwendungen. Tellus, 8: 287—300.

Harper, B.A. Sobey, R.J. and Stark, K.P., 1977. Numerical simulation of tropical cyclone storm surge along the Queensland coast, Parts I—X. Department of Civil and Systems Engineering, James Cook University.

Heaps, N.S., 1969. A two-dimensional numerical sea model. Proc. R. Soc. London, Ser. A, 265: 93—137.

Jelesnianski, C.P., 1965. A numerical calculation of storm tides induced by a tropical storm impinging on a continental shelf. Month. Weather Rev., 93: 343—358.

Jelesnianski, C.P., 1972. SPLASH (Special Program to List Amplitudes of Surges from Hurricanes) — I. Landfall Storms. NOAA Technical Memorandum NWS TDL-46.

Jelesnianski, C.P., 1974. SPLASH (Special Program to List Amplitudes of Surges from Hurricanes) — II. Geneal Track and Variant Storm Conditions. NOAA Technical Memorandum NWS TDL-52.

Leendertse, J.J., 1967. Aspects of a computational model for long-period water-wave propagation. Rand Corporation. RM-5294-PR, Santa Monica.

Pearce, B.R. and Pagenkopf, J.R., 1975. Numerical calculation of storm surges: An evaluation of techniques. Proc. 7th Annu. Offshore Technol. Con., Houston, Texas, pp. 887—901.

Reid, R.O. and Bodine, B.R., 1968. Numerical model for storm surges in Galveston Bay. J. Waterways Harbors Div. ASCE, 94: 33—57.

Sobey, R.J., Harper, B.A. and Stark, K.P., 1977. Numerical simulation of tropical cyclone storm surge. Department of Civil and Systems Engineering, Research Bulletin No. CS14, James Cook University.

Sobey, R.J., Harper, B.A. and Mitchell, G.M., 1982. Numerical modelling of tropical cyclone storm surge. Civ. Eng. Trans. Inst. Eng., Aust., CE24: 151—161. (See also Proc. 17th Int. Conf. Coastal Eng., ASCE, Sydney, 1, pp. 725—745, 1980.)

Taylor, C. and Davis, J., 1975. Tidal and long wave propagation — a finite element approach. Computers Fluids, 3: 125—148.

Welander, P., 1964. Numerical prediction of storm surges. Adv. Geophys., 8: 315—379.

Wu, J., 1969. Wind stress and surface roughness at air—sea interface. J. Geophys. Res., 74: 444—455.